



Explorative studies for the development of fast He beam plasma diagnostics

S. Menhart ^{a,*}, M. Proschek ^a, H.-D. Falter ^a, H. Anderson ^b, H. Summers ^b,
A. Staebler ^c, P. Franzen ^c, H. Meister ^c, J. Schweinzer ^c, T.T.C. Jones ^d, S. Cox ^d,
N. Hawkes ^d, F. Aumayr ^a, H.P. Winter ^a

^a *Institut für Allgemeine Physik, Wiedner Hauptstraße 8-10, TU Wien, A-1040 Vienna (Association EURATOM-OEAW), Austria*

^b *Department of Physics and Applied Physics, University of Strathclyde, Glasgow, UK*

^c *IPP Max-Planck-Institut für Plasmaphysik, D-85748 Garching, Germany*

^d *JET Joint Undertaking, Abingdon, Oxfordshire OX14 3EA, UK*

Abstract

Modelling calculations for a fast He beam on its way through a tokamak plasma have been performed at TU Wien. They are based on the collisional-radiative ADAS model for He beams which delivers radially resolved population density and line intensity profiles for any initial population of a diagnostic He beam and any plasma structure. The effect of the metastable triplet population in the incident beam on the line emission profiles is shown. A sensitivity study of the optical lines with respect to electron temperature and density has been performed in the plasma edge and core regions. To validate these model calculations, experiments using fast He beams and beam emission spectroscopy have been performed at ASDEX Upgrade (IPP Garching) and JET by injecting He gas into the ion sources of the H- or D-heating beam systems. © 2001 Elsevier Science B.V. All rights reserved.

Keywords: Plasma modelling; Collisional-radiative model; Diagnostic He beam; Beam emission spectroscopy

1. Motivation

A precise knowledge of the temperature and density profiles of edge and internal transport barriers [1,2] is essential for both plasma transport modelling and evaluating plasma stability. During the last years, beam emission spectroscopy utilizing fast Li beams of several 10 keV energy [3,4] or thermal He beams [5] have become well established tools for determining electron density (Li, He) and electron temperature profiles (He). These diagnostic methods measure the emission from injected neutral particles excited by collisions with plasma particles. Both thermal He and Li beams do not penetrate far beyond the scrape-off layer in the dense plasmas of larger tokamaks. Fast (≤ 10 keV) He beams

penetrate much further into the plasma than either thermal He or Li beams of comparable energy. Moreover, He beams can also be used as electron donors for charge exchange spectroscopy as plasma ion temperature and density diagnostics. One important goal of our investigations is to determine whether the emission from fast He beams retains sufficient sensitivity on temperature variation to be usable as temperature diagnostics.

In the next section, we describe the modelling required for interpretation of the He beam emission.

2. The collisional-radiative model

Several collisional-radiative models ('cr-models') have been developed for thermal He beams [5,6]. At such low beam energy ion collisions can be neglected. In the case of thermal beams, the path length the beam requires to adjust to local variations in the plasma parameters is small compared to the length over which

* Corresponding author. Tel.: +43-1 58801 13486; fax: +43-1 58801 13499.

E-mail address: menhart@iap.tuwien.ac.at (S. Menhart).

plasma parameters change significantly. For these ‘relaxed states’ HeI-line ratios can be identified which are dominated by either electron density or temperature.

The line emission of fast He atoms in a plasma has been modelled previously by several groups [7,8] by adding ion-impact excitation and ionisation. Recently, a cr-model for He beams (ADAS311, ADAS313) has been developed by the ADAS group at the University of Strathclyde, Glasgow [9], which takes into account electron and ion impact excitation, de-excitation, ionisation, charge exchange between He and fully stripped ions, and spontaneous emission from excited He states.

The local population density N_i of atoms in state i of a He beam penetrating a plasma can be determined by stepwise solving the balance equations, which can be written in matrix form

$$v_b \frac{dN_i}{dx} = \sum_j C_{ij} N_j, \quad (1)$$

where C_{ij} is called the collisional-radiative matrix, which includes all the collisional and spontaneous emission contributions mentioned above, v_b is the beam velocity. The matrix elements C_{ij} are functions of electron and ion temperature (T_e, T_i), electron and ion density (n_e, n_i) and beam energy (E_b). ADAS311 assembles the balance equations up to an arbitrary principal quantum number n . Levels up to an adjustable threshold n' are treated as ‘nls-resolved’, levels with $n > n'$ are treated as ‘ns-resolved’, i.e., levels with the same principal and spin quantum number are merged. In our calculations n' was chosen to be 5, the maximum principal quantum number n was 110. In the first version of ADAS311, which has been used for our calculations, the excited states are treated as being in equilibrium with the ground state (1^1S) and the two metastable states (2^1S and 2^3S). The balance equations are reduced by using so-called ‘condensation techniques’ [9] to

$$\begin{aligned} v_b \frac{dN_{1^1S}}{dx} &= -n_e S_{1^1S} N_{1^1S} + n_e S_{2^1S \rightarrow 1^1S} N_{2^1S} + n_e S_{2^3S \rightarrow 1^1S} N_{2^3S}, \\ v_b \frac{dN_{2^1S}}{dx} &= n_e S_{1^1S \rightarrow 2^1S} N_{1^1S} - n_e S_{2^1S} N_{2^1S} + n_e S_{2^3S \rightarrow 2^1S} N_{2^3S}, \\ v_b \frac{dN_{2^3S}}{dx} &= n_e S_{1^1S \rightarrow 2^3S} N_{1^1S} + n_e S_{2^1S \rightarrow 2^3S} N_{2^1S} - n_e S_{2^3S} N_{2^3S}, \end{aligned} \quad (2)$$

n_e denotes the electron density, S_i the total loss from the non-equilibrium level i , $S_{i \rightarrow j}$ stands for the excitation from level i to level j , including all stepwise processes via excited states. These nine coefficients are called ‘generalized radiative coefficients’ (GRCs). For assessing the progression of the three levels, one has to deal only with a (3,3)-matrix. Furthermore, electron and ion temperature are considered to be equal in ADAS311. The above simplifications are justified for

plasma temperatures small compared to the energy of the injected atoms. Experimental and theoretical cross-sections, rate coefficients and spontaneous emission coefficients for levels up to $n = 4$ are stored in ADAS. Various approximation methods are used for calculating the rate coefficients not contained in the ADAS database [10]. The ADAS code provides the GRCs for a predefined list of plasma temperatures, densities, and beam energies. Furthermore, for emission lines of interest so-called ‘effective beam emission coefficients’ (EECs) for each non-equilibrium level are calculated. These EECs enable for deduction of the line intensity profiles from the population-density profiles of the non-equilibrium levels. The code SCOTTIE, developed at IAP (TU Wien), numerically solves Eq. (2) by using GRCs and EECs from ADAS. The input for SCOTTIE are the electron density and temperature profile, the beam energy, beam equivalent current and diameter, initial beam composition (1^1S , 2^1S , and 2^3S), and the step increment.

3. Predictions for tokamak plasmas

The beam emission has been modelled for typical ASDEX Upgrade (‘AUG’)- and JET discharges using a neutral beam current of 1 A uniformly distributed over a diameter of 0.1 m ($\hat{=} 127 \text{ A/m}^2$). The beam energy was taken in accordance with the energy available for the experiments. Both incident pure 1^1S and pure 2^3S beams have been used for modelling. The results for a beam with a metastable fraction between these two extremes can be determined by mixing the two results with the corresponding weight factors. The line emission intensity profiles have been calculated for all lines in the wavelength region 389–728 nm, i.e., six singlet and five triplet lines.

3.1. AUG discharge #11277

For AUG, we use shot #11277 with a line averaged density of $8 \times 10^{19} \text{ m}^{-2}$ and a peak electron temperature of 1.8 keV as inputs for our modelling. The He beam energy is 30 keV. As all lines of one spin system show rather similar behaviour, only the most intense lines of each spin system are represented in Fig. 1 which shows the radial variation of the non-equilibrium level populations and the emission profile of the strongest singlet and triplet line for an initially pure 1^1S and pure 2^3S beam, respectively.

After passing through the entire plasma the pure 1^1S beam is attenuated to 5% of its incident current density. The 2^1S population density is strongly coupled to the 1^1S population density.

The 2^3S population density shows a quite different behaviour. The 2^3S state is preferably populated in regions with low temperatures (near the separatrix) and

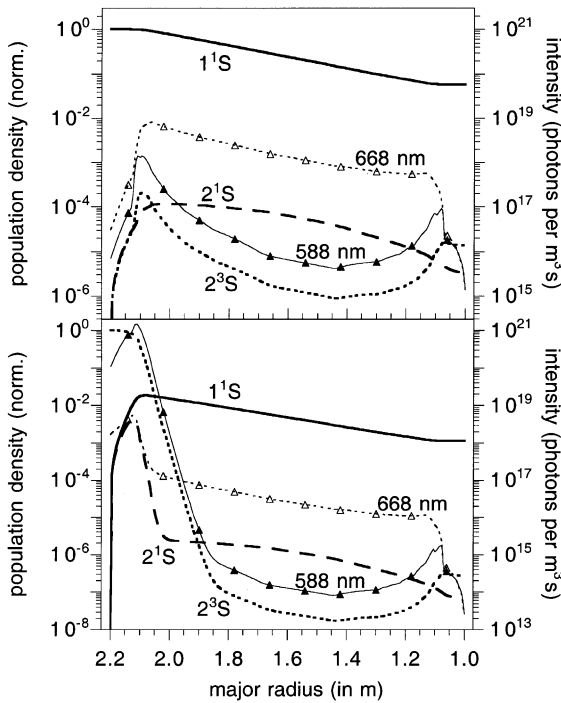


Fig. 1. Progression of the 1^1S , 2^1S and 2^3S populations and the most intense singlet (668 nm) and triplet (588 nm) lines for an initially pure 1^1S (top) and 2^3S beam (bottom), respectively. The modelling is based on AUG discharge #11277 and a 1 A/30 keV He beam with 0.1 m diameter.

strongly depopulated in the hot core. The line profiles are quite similar to the corresponding metastable population density profiles.

The initially pure 2^3S beam decays with an e-folding length of 17 mm, after which a population density composition independent from the initial beam composition is reached. This means that for such a situation the initial beam composition has no influence on the beam composition in the core plasma. In the case of an initially pure 2^3S beam, the 2^3S concentration in the plasma core is by almost two orders of magnitude lower than in the case of an initially pure ground state beam. This can be explained by the strong beam attenuation in the case of the pure 2^3S beam, reducing the beam flux by two orders of magnitude within the first 0.1 m. Again, the line intensity profiles reflect the corresponding metastable state profiles.

3.2. JET discharge #42676

For a typical JET plasma, we use discharge #42676 (H-mode, line averaged density $3.6 \times 10^{20} \text{ m}^{-2}$, maximum electron temperature 5 keV) and a beam energy of 80 keV. As with the calculations for AUG, all lines of a

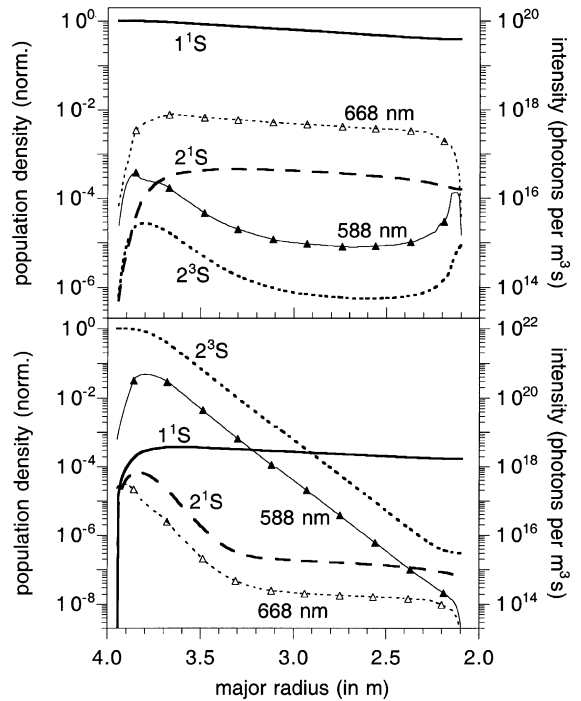


Fig. 2. Progression of the 1^1S , 2^1S and 2^3S populations and the most intense singlet (668 nm) and triplet (588 nm) lines for an initially pure 1^1S (top) and 2^3S beam (bottom), respectively. The modelling is based on JET discharge #42676 and a 1 A/80 keV He beam with 0.1 m diameter.

given spin system show rather similar behaviour. Hence, only the most intense lines of either spin system are shown in Fig. 2 for initially pure 1^1S and pure 2^3S beams, respectively.

Compared to AUG, the higher beam energy and electron temperature leads to a reduced attenuation and repopulation of the beam despite the higher line averaged density at JET. After passing the entire plasma the pure 1^1S beam is attenuated to only 40% of its initial beam density. As for the AUG calculations, the 2^1S population density is strongly coupled to the 1^1S population density, whereas the 2^3S population density shows enhanced population in regions with low temperatures and a strong depopulation in the hot core. The line profiles are quite similar to the corresponding metastable population density profiles. All 11 lines are stronger than the minimum intensity needed for observation, which were obtained from spectrometer geometry and sensitivity estimates.

The e-folding length for the decay of the 2^3S population is with 0.1 m about a factor of six larger than in the case of the AUG discharge. At each point on the beam path the beam composition depends on the initial beam composition.

4. Sensitivity study

To assess the potential of He beam emission spectroscopy for temperature and density diagnostics, a JET ITB discharge (shot #40554) was modelled using smooth temperature and density profiles, or density, respectively, temperature profiles with steps and constant sections. This was done before and after the formation of the ITB. The response of the emitted intensity $\Delta I/I$, normalized to the density ($\Delta n/n$) or temperature step ($\Delta T/T$), respectively, for an 80 keV He beam with an initial 2^3S fraction of 10% is shown in Table 1 for some characteristic lines.

The sensitivity to density is good for basically all lines, the sensitivity to temperature is large enough to be evaluated, however, it varies from line to line and even can change sign with the formation of an ITB. This means that the sensitivity to both temperature and density is adequate. A suitable procedure to derive temperature and density profiles from the measured HeI emission profiles has still to be developed.

5. Experiments at AUG and JET

For the experiments at AUG a pure 30 keV He atom beam with an equivalent current of 14 A was produced by running one of the neutral beam injectors with He instead of deuterium for up to 300 ms. All HeI lines in the visible range were measured with either the standard CER spectrometer using 16 lines of sight or a spare spectrometer with four lines of sight. For a suitable evaluation the Doppler shifted intensity has to be identified. This was only possible with a few spectra taken with the CER spectrometer.

Table 1

Relative intensity changes for two singlet (668, 505 nm) and two triplet emission lines (389, 588 nm) for density and temperature changes

Major radius (m)	668 nm	505 nm	389 nm	588 nm
<i>($\Delta I/I$)/($\Delta n/n$) before ITB formation</i>				
4.26	0.73	0.41	0.22	0.40
4.08	0.73	0.28	0.13	0.40
3.93	0.73	0.13	0.91	0.48
<i>($\Delta I/I$)/($\Delta T/T$) before ITB formation</i>				
4.26	0.26	0.11	0.13	0.31
4.08	0.17	0.00	0.16	0.34
3.93	0.03	0.08	0.49	0.75
<i>($\Delta I/I$)/($\Delta T/T$) after ITB formation</i>				
4.26	-0.23	-0.10	0.16	-0.21
4.08	-0.15	0.00	0.20	-0.18
3.93	-0.02	0.10	0.20	-0.12

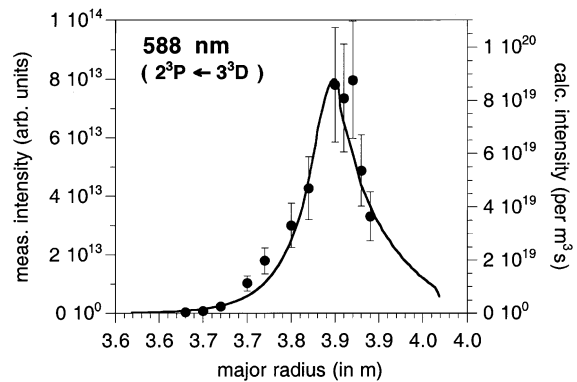


Fig. 3. Comparison of the measured (circles) and calculated (solid line, assuming 10% 2^3S fraction) line emission at 588 nm for JET discharge #49504.

Similar experiments have been performed at JET. Here a so-called ‘doped’ He beam, i.e., a neutral deuterium heating beam with a small He fraction was injected into the plasma. This provided a 75 keV beam with typically 4 A equivalent current and a 2^3S fraction in the order of 10%, as the He ion beam was neutralized in D_2 gas.

Fig. 3 shows the comparison between an experiment performed at JET (shot #49504) and the corresponding model calculation results, using density and temperature profiles measured with the respective standard diagnostics (KG1, LIDAR). The observed emission lines are well represented by the model calculations. Further similar experiments are planned at both AUG and JET.

6. Conclusions

Model calculations performed for typical AUG and JET discharges showed that for fast neutral He beams with equivalent currents of several A, the line intensities of the most intense lines of both the singlet and the triplet system are sufficiently strong for evaluation. This has been verified by experiments at both setups. Most visible lines show sufficient sensitivity on electron density and temperature. It is, therefore, expected that fast He beam emission spectroscopy can be used for temperature and density diagnostics as the HeI lines show an adequate sensitivity for both parameters. However, appropriate routines to extract profiles of density and temperature from the measured emission profiles have still to be developed.

Acknowledgements

S.M. and M.P. have been supported by Friedrich Schiedel-Stiftung für Energietechnik, Vienna.

References

- [1] P. Breger et al., Plasma Phys. Control. Fusion 40 (1998) 347.
- [2] X. Litaudon et al., JET-P(98)41, JET Joint Undertaking, UK, 1998.
- [3] R. Brandenburg, Lithiumstrahldiagnostik von Kernfusionsplasmen, PhD thesis, TU Wien, 1998 (unpublished).
- [4] J. Schweinzer et al., Plasma Phys. Control. Fusion 34 (1992) 1173.
- [5] M. Brix, Messung von Elektronentemperatur und -dichte mittels Heliumstrahldiagnostik im Randschichtplasma eines Tokamaks, PhD thesis, Ruhr-Universität Bochum, 1998 (unpublished).
- [6] S. Sasaki et al., Rev. Sci. Instrum. 67 (1996) 3521.
- [7] A.A. Korotkov, R.K. Janev, Phys. Plasmas 3 (1996) 1512.
- [8] M. Brix, Abschlußbericht zum Forschungsauftrag Nr. 021/41362607/930 an die Forschungszentrum Jülich GmbH, 1999.
- [9] H.P. Summers, Atomic Data and Analysis Structure, User Manual, Internal Report, JET-IR (94) 06, JET Joint Undertaking, UK, 1994.
- [10] H. Anderson, PhD thesis, Univ. of Strathclyde, Glasgow, 1999 (unpublished).